Nano Research 2014, 7(3): 365–379
DOI 10.1007/s12274-013-0402-y
Research Article

ISSN 1998-0124
CN 11-5974/O4

Mechanistic study of substrate-based galvanic replacement reactions

Kyle D. Gilroy, Aarthi Sundar, Pouyan Farzinpour, Robert A. Hughes, and Svetlana Neretina (✉)

College of Engineering, Temple University, Philadelphia 19122, USA

Received: 11 October 2013
Revised: 13 December 2013
Accepted: 15 December 2013

KEYWORDS
galvanic replacement reaction,
hollow metal nanoshells,
nanocages,
heteroepitaxy,
stacking faults

ABSTRACT

The sacrificial templates used in galvanic replacement reactions dictate the properties of the hollow metal nanostructures formed. Here, we demonstrate that substrate-based Au–Ag nanoshells with radically altered properties are obtained by merely coating silver templates with an ultrathin layer of gold prior to their insertion into the reaction vessel. The so-formed nanoshells exhibit much smoother surfaces, a higher degree of crystallinity and are far more robust. Dealloying the nanoshells results in the first demonstration of substrate-based nanocages. Such cages exhibit a well-defined pattern of geometric openings in directions corresponding to the {111}-facets of the starting template material. The ability to engineer the cage geometry through adjustments to the orientational relationship between the crystal structure of the starting template and that of underlying substrate is demonstrated. Together these discoveries provide the framework to advance our understanding of the mechanisms governing substrate-based galvanic replacement reactions.

1 Introduction

Water-based synthetic protocols utilizing galvanic replacement provide straightforward pathways for fabricating hollow metal nanoshells [1, 2]. Such reactions proceed by reacting preformed sacrificial metal templates with noble metal salts exhibiting a higher electrochemical potential. The reaction, which occurs spontaneously, sees the oxidation and dissolution of metal atoms from the template as metal ions are reduced and deposited on its surface. The product of the reaction is a nanostructure of greater complexity than the sacrificial template. It typically features a hollowed morphology, although notable exceptions have been identified [3–5]. The prototypical galvanic replacement reaction is one where silver templates are reacted in an aqueous solution of $HAuCl_4$ [6]. In this reaction, the reduction of each Au^{3+} ion results in the oxidation and dissolution of three Ag^{+} ions from the template. With both deposition and dissolution being highly dependent on the size, shape and crystallinity of the silver template, numerous synthetic strategies are emerging in an effort to engineer nanomaterials for use in biomedical [2, 7], sensor [8–11]

Address correspondence to neretina@temple.edu

and catalytic applications [12, 13]. Coinciding with this effort are fundamental studies aimed at elucidating the mechanisms governing galvanic replacement reactions [4, 14–18].

Silver nanocubes exhibiting six {100}-facets are, from a mechanistic standpoint, the simplest template material. Galvanic replacement reactions transform the nanocube into a hollow nanobox composed of a Au–Ag alloy [14]. If, however, the reaction is allowed to continue after the nanobox has formed the structure undergoes morphological transformations, first through the formation of square pores on the cube faces (i.e., a nanocage) and then through fragmentation. Coinciding with this deconstruction is a composition which trends toward pure Au. Many aspects of this progression are well understood. The initial stages of the reaction are characterized by the dissolution of Ag from the surface of the cube as Au is heteroepitaxially deposited. The 100 °C reaction temperature, needed to prevent the precipitation of AgCl [19], is sufficient to cause rapid alloying between the deposited Au and the underlying Ag. Template hollowing initiates at a single defect site on one of the six faces of the nanocube. As Au continues to plate the cube the exiting Ag^+ first results in the formation of a pit and then hollows out the interior of the structure until the supply of pure Ag is exhausted. The side-opening then seals due to volume diffusion, surface diffusion, dissolution followed by re-deposition or a combination of the aforementioned [2]. At this stage the nanostructure exists as an alloyed Au–Ag nanobox, a structure which preserves the original shape of the template. Longer reaction times lead to a continuation of the galvanic replacement reaction through the dealloying of Ag from the walls of the nanobox [14]. Because of the 1:3 Au:Ag replacement ratio, dealloying results in the injection of vacancies and an overall reduction in the number of atoms in the structure. Vacancy coalescence eventually leads to the formation of square pores in the sidewalls of the structure. Continuing the reaction leads to nanostructure fragmentation which results from further dealloying and Ostwald ripening processes.

When templates exhibiting complex faceted geometries are used in galvanic replacement reactions they promote a facet dependent reactivity. As a result, the reaction product can achieve a shape which radically differs from that of the original template. Notable examples include templates which are cuboctahedrons [3, 20, 21], polyhedrons [4], multiply twinned particles (MTP) [15], and nanowires [22]. The early stages of the reaction are characterized by the preferential deposition of Au on facets having high surface energy. With a hierarchy of surface energies of $\gamma\{110\} > \gamma\{100\} > \gamma\{111\}$, the deposition tends to accentuate the {110}- and {100}-facets at the expense of {111}-facets. With preferential deposition occurring along high surface energy facets, the low surface energy {111}-facets typically become the locations for pitting, hollowing and dealloying-induced void formation [1]. Noteworthy, is that the preferential deposition tends to increase the surface energy of the emerging structure, a behavior that is in opposition to thermal diffusion processes [23] which favor the formation of low surface energy {111}-facets.

Previously, we carried out galvanic replacement reactions on substrate-based silver templates which share a heteroepitaxial relationship with the underlying substrate [24]. The ability to form a nanohut structure which takes the form of a near-hemispherical Au–Ag nanoshell that faces downward on the surface of the substrate and which has a single opening near its base was demonstrated. The nanohuts, however, exhibit a rough surface morphology consisting of many loosely connected lobes. Motivated by previous studies on solution-dispersed templates which demonstrate the importance of alloying, pitting and facet-selective deposition in the early stages of the replacement process we undertook an investigation which altered the start of the reaction by coating the substrate-based silver templates with a 3 nm thick layer of Au prior to their insertion into the reaction vessel. Here, we report that such a layer dramatically alters the product of reaction, yielding nanoshells which (i) exhibit a much smoother surface morphology, (ii) preserve the general shape of the starting template, (iii) are far more robust and (iv) dealloy in a manner yielding a variety of unique nanocage geometries. The discovery is used to advance the understanding of substrate-based galvanic replacement reactions.

2 Results

Silver templates for galvanic replacement reactions were fabricated on (0001)-oriented sapphire substrates using dynamic templating, a lithography-free templated assembly route which we describe in detail elsewhere [25]. When complete, the process yields a periodic array of Ag templates with diameters of 270 nm. The majority of the templates, while still appearing quite rounded, show faceting consistent with either [110]- or [111]-oriented substrate-truncated cuboctahedrons [23], but where [100]- and [211]-oriented templates also appear in significant numbers. Substrate-based galvanic replacement reactions [24] utilizing an aqueous $HAuCl_4$ solution were then carried out on these Ag templates as well as on identical templates which were first sputter coated with 3 nm of Au prior to reaction. The coating is smooth and follows the contours of the underlying template (Fig. S1 in the Electronic Supplementary Material (ESM)).

Figure 1 compares the nanoshells derived from silver templates with those obtained from Au-coated silver templates. In both cases, scanning electron microscopy (SEM) images reveal that the galvanic replacement reactions transformed the template structures into periodic arrays of hollow nanoshells. Striking differences, however, are observed when comparing the morphology of the nanoshells obtained. Nanoshells derived from the silver templates (Fig. 1(a)) exhibit an irregular surface morphology consisting of numerous loosely connected lobes. This rough morphology is observed even when the reaction is carried out at a slower rate (Fig. S2 in the ESM). In contrast, the Au-coated silver templates (Fig. 1(b)) yield nanoshells which exhibit a much smoother outer surface with an opening adjacent to the substrate. This opening can have a hexagonal geometry (inset to Fig. 1(b)), although openings with jagged irregular edges are more typical. For both cases, energy dispersive X-ray spectroscopy (EDS) measurements reveal a nanoshell composition of near $Au_{0.70}Ag_{0.30}$.

The transfer of the nanoshells from the substrate surface to transmission electron microscopy (TEM) grids allowed for the inner surfaces of the nanoshells to be imaged. Figures 1(c) and 1(d) show top- and side-view TEM images of inverted nanoshells (i.e., nanobowls [26–29]) derived from the uncoated and Au-coated silver templates, respectively. The images obtained confirm that the structures are hollow with a shell thickness below 40 nm. Also noteworthy is the fact that the nanoshells are quite robust, maintaining their structural integrity during the removal process. Unique to the nanoshells derived from the Au-coated silver template is series of parallel planar defects

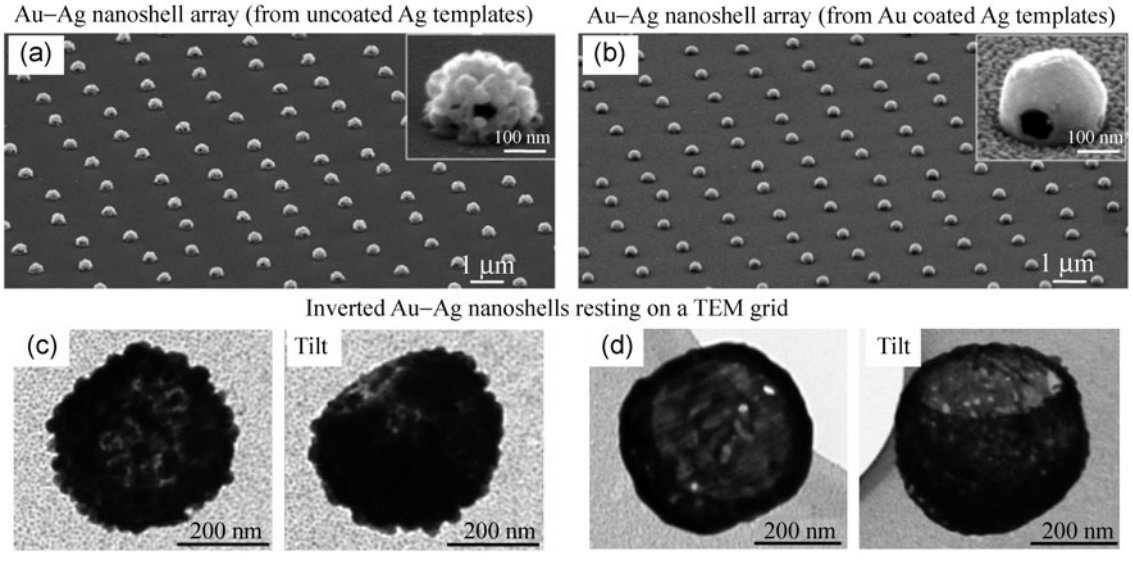

Figure 1 65° tilted-view SEM images of a nanoshell array produced using galvanic replacement reactions on (a) silver templates and (b) silver templates coated with 3 nm of Au. The insets show a high magnification view of an individual nanoshell. Top- and tilted-view TEM images of inverted nanoshells obtained from silver templates having the (c) uncoated and (d) Au-coated configurations.

extending from one side of the shell to the other (Fig. 1(d)).

The temporal evolution of the sacrificial templates into hollow nanoshells was assessed for the uncoated and Au-coated template configurations. Figures 2(a)–2(d) show SEM images of uncoated templates exposed to aqueous $HAuCl_4$ for time intervals ranging from 4 to 30 min. The early stages of the reaction result in the preferential deposition of Au onto the high curvature surfaces where facets intersect. This in combination with a slower rate of deposition onto the {100} and {111} facets exaggerates the underlying crystallography of the substrate-truncated cuboctahedron (Fig. 2(a)). Noteworthy is the fact that the resulting framework is disconnected at numerous locations. As the reaction proceeds the framework becomes increasingly rough, developing lobes while the facets of the structure remain smooth (Fig. 2(b)). As the lobes continue to become more pronounced, prominent openings emerge in the structure (Fig. 2(c)). While somewhat obscured by the lobes, an examination of a large number of structures makes it apparent that the openings consistently form at the facet positions of the initial Ag template, a behavior consistent with the dealloying process. Reactions allowed to proceed further result in structures where the pattern of

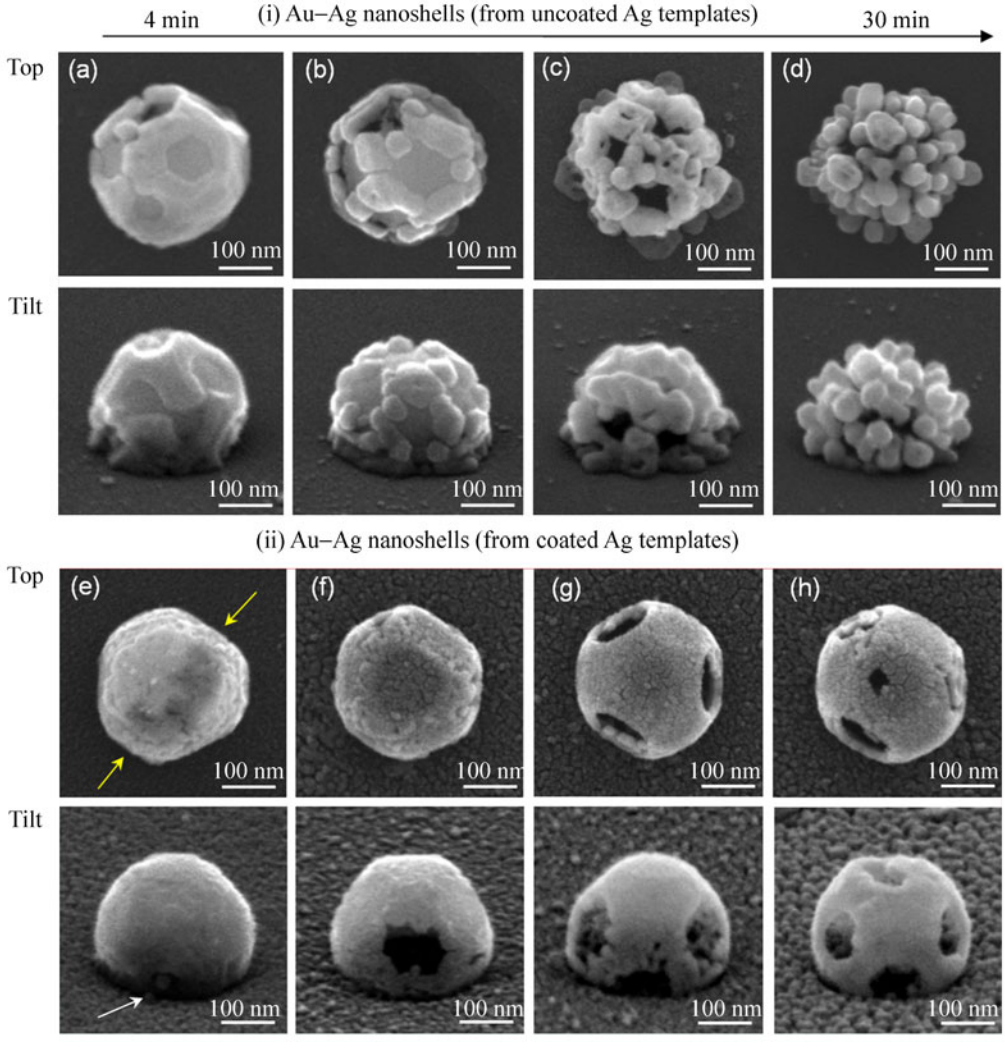

Figure 2 Top- and 65° tilted-view SEM images showing the evolution of (i) silver templates and (ii) silver templates coated with 3 nm of Au as they undergo galvanic replacement reactions for time intervals ranging from 4 to 30 min. It should be noted that the darker contrast in the top-view SEM image shown in Fig. 2(e) reveals the existence of a hollow channel within the structure (denoted by yellow arrows).

openings is further obscured by an increase in the overall porosity and the continued development of lobes (Fig. 2(d)).

The progression for galvanic replacement reactions carried out on Au-coated silver templates is markedly different. Figures 2(e)–2(h) show this progression for nanoshells derived from [111]-oriented templates. The early stage morphology of the nanoshell derived from the Au-coated template (Fig. 2(e)) is characterized by an exceedingly smooth shell with a small pinhole near the base of the structure (denoted by the white array) and a single hollow channel extending from one side of the template to the other (denoted by yellow arrows). Such channels are consistently observed for templates that are not fully reacted. The fact that many of the channels in adjacent structures are parallel to each other (Fig. S3 in the ESM) suggests a correlation between the channel direction and the underlying crystal structure of the silver template. In striking contrast to the structures derived from uncoated templates, those utilizing Au-coated silver templates do not undergo a rapid deterioration in their morphology for longer reaction times. Instead the Au deposition occurs in a far more uniform manner over the entire template, showing only a slight preference for deposition on {100} facets and along the curved regions where the facets meet (Fig. 2(f)). At this point the structure has also developed a single large opening at its base. This is followed by a progression which transforms the structure into a nanocage [1], a designation attributed to hollow structures with a geometric pattern of openings over their surface (Figs. 2(g) and 2(h)). This late-stage behavior is consistent with the dealloying process.

Further insights into the dealloying process are obtained by comparing SEM images for nanoshells derived from templates of various orientations. Figure 3 shows the early and late stages of the dealloying process for [100]-, [110]-, [111]-, and [211]-oriented structures where the structure orientation is assigned based on faceting consistent with a substrate-truncated cuboctahedron. The early stages show the formation of small openings on the {111} facets near the base of the structure. Other {111} facets show contrast consistent with being thinner than the remainder of the structure, a feature consistent with a galvanic replacement process that deposits more slowly on low surface energy facets. It is noted that the openings often appear as triangular features as denoted by the yellow arrow in Fig. 3(a), a feature analogous to the square openings observed in the dealloying of solution-based nanoboxes [14]. The late stages of the dealloying process consistently give rise to a nanocage geometry with a pattern of openings corresponding to the {111} facets of each uniquely oriented structure. The fact that each of these nanocage structures is unique, demonstrates the potential to engineer the cage geometry based on the orientational relationship between the crystal structure of the initial template and the substrate. Individual structures do, however, show a degree of variability in the number of {111} facets which develop openings. The observed trend, however, is for openings to appear most frequently at the base of the structure, while those closer to the top are less common. <111>-oriented openings are commonly observed in late stage galvanic replacement reactions carried out on solution-dispersed templates and are typically attributed to an Ostwald ripening process [2]. Unique to these substrate-based structures is that many of the openings often express the hexagonal geometry exhibited by the six-fold symmetry of a (111) plane.

As previously mentioned, the early stages of galvanic replacement reactions carried out on Au-coated silver templates are characterized by template hollowing which proceeds along a channel whose direction is determined by the underlying crystal structure of the template. In order to further investigate this phenomenon processing conditions were established which allowed randomly positioned silver templates to assemble directly on Si_3N_4 TEM grids. The grid with templates was then exposed to the galvanic replacement reaction. The so-formed Ag islands have a broad size distribution and a diverse range of faceting. They form with the [211]-, [111]-, [100]-, or [110]-orientation normal to the surface of the grid, where the [211]-orientation is by far the most common. The varied nature of these templates provided an excellent platform for characterizing nanoshells derived from a diverse collection of templates all exposed to

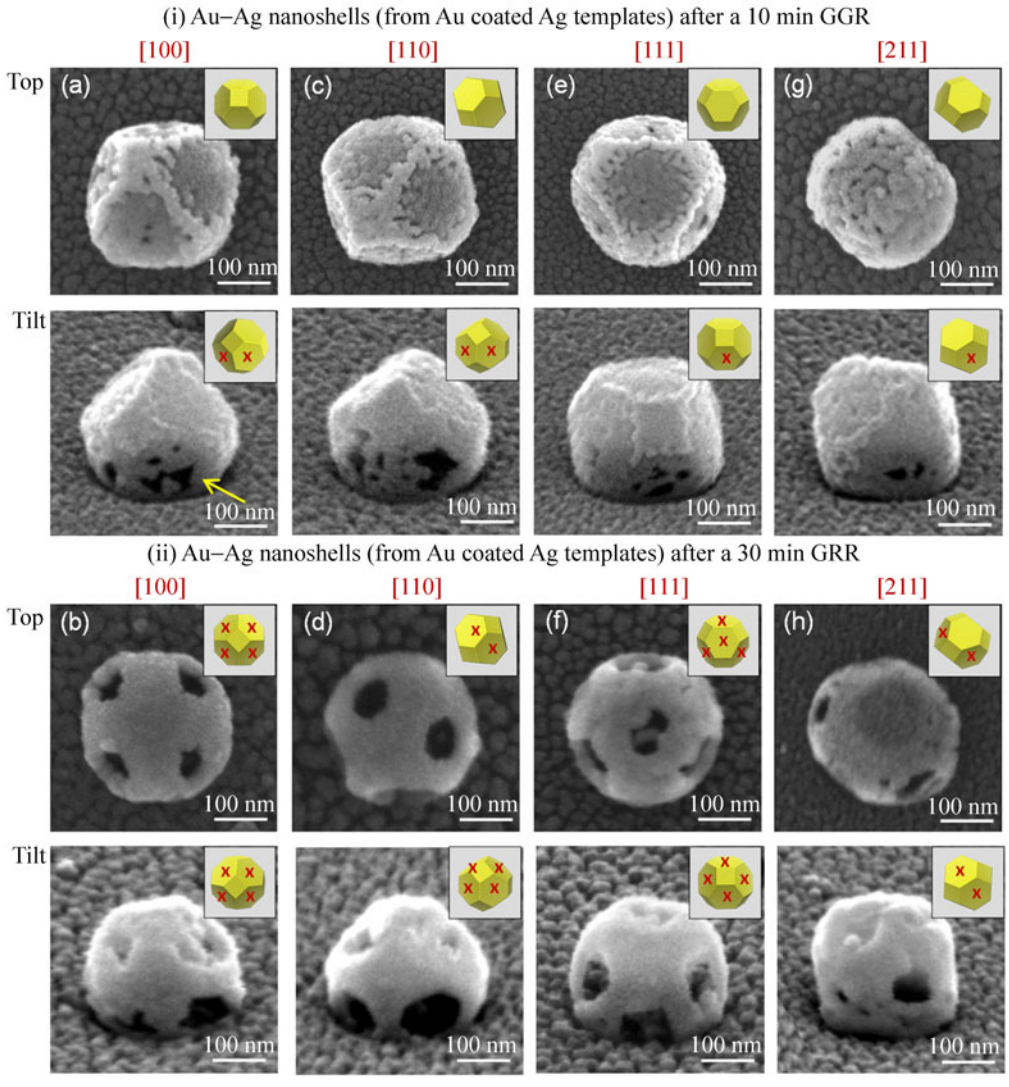

Figure 3 Top- and 65° tilted-view SEM images showing the evolution of structures from Au–Ag (i) nanoshells to (ii) nanocages. This dealloying process is shown for structures derived from Au-coated silver templates having a (a) and (b) [100]-, (c) and (d) [110]-, (e) and (f) [111]-, and (g) and (h) [211]-orientation. Note that each orientation gives rise to a unique nanocage geometry. The insets to the figures show schematics of top- and side-view cuboctahedrons with the same orientation as the nanoshell. The {111} facets denoted by an "x" show a partial or complete opening.

the same galvanic replacement reaction.

Figure 4 shows TEM images and the corresponding selected area electron diffraction (SAED) pattern for a [110]-oriented silver template and nanoshells derived from a galvanic replacement reaction which exposed both uncoated and Au-coated silver templates to a 15 μM $HAuCl_4$ solution for 10 min. In both cases, the nanoshells appear quite similar to those formed on sapphire substrates, a result which validates the Si_3N_4-based assembly process. Electron diffraction for the uncoated sample reveals the expected single-crystal reflections superimposed on a polycrystalline diffraction pattern (Fig. 4(b)). The pattern is consistent with a structure having a dominant [110]-orientation normal to the Si_3Ni_4 surface, but where parts of the structure have a polycrystalline character. In contrast, the coated nanoshell reveals single crystal reflections consistent with a [110]-orientation normal to surface (Fig. 4(c)). The result demonstrates that the Au-coated templates give rise to nanoshells with a higher degree of crystallinity.

Figure 5 shows plan view TEM images and the corresponding SAED patterns for samples derived from Au-coated silver templates with varying degrees

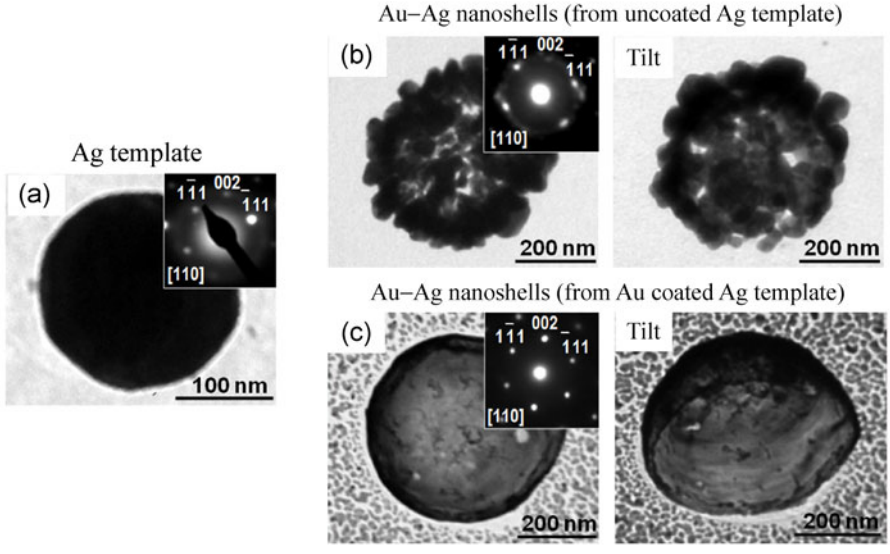

Figure 4 TEM images and the associated SAED patterns for a (a) [110]-oriented silver template and [110]-oriented nanoshells derived from (b) uncoated and (c) Au-coated silver templates. The thin discontinuous Au film encircling the shells in Fig. 4(c) is a remnant of the template coating process. The tilt angle is 35°.

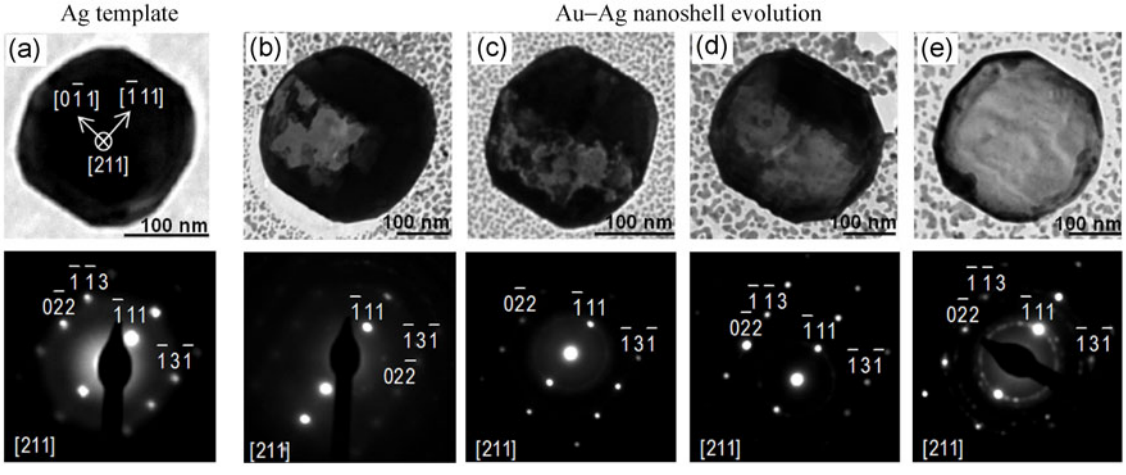

Figure 5 TEM images and the corresponding SAED patterns of (a) a [211]-oriented silver template and (b)–(e) similarly shaped templates with varying degrees of hollowing due to the galvanic replacement reaction. Note that the replacement reaction proceeds through the formation of a channel which first extends from one side of the Ag template to the other followed by an expansion in width.

of hollowing resulting from the termination of the replacement reaction before completion. A particular [211]-oriented structure exhibiting a distinctive shape was targeted due to its high rate of occurrence on the Si_3N_4 substrate. The unreacted template (Fig. 5(a)) has two prominent parallel facets which correspond to the in-plane [$\bar{1}$11]-direction. It should be noted that face centered cubic (fcc) crystal structures are prone to the formation of {111} facets since this plane has the lowest surface energy [30]. The early stages of the replacement process are characterized by the formation of a hollowed channel (Fig. 5(b)) which appears as a bright rectangular feature along the [0$\bar{1}$1]-direction and is, thus, parallel to the ($\bar{1}$11) facets of the particle. Continued hollowing results in a channel which extends from one side of the structure to the other (Fig. 5(c)). This is followed by a widening of the channel (Fig. 5(d)) until the hollowing process is complete (Fig. 5(e)). Of significance is the fact that the diffraction patterns appear similar throughout the replacement process. With Au and Ag sharing the same fcc crystal structure and having nearly the same

lattice constant (Ag: a = 4.085 Å, Au: a = 4.078 Å), the diffraction pattern is not expected to change appreciably, provided that Au deposits heteroepitaxially on the template during the galvanic replacement reaction. While the epitaxial nature of the replacement process has been previously documented [3, 14], it is noteworthy that epitaxy is not disrupted by the room temperature deposition of 3 nm of Au on top of the silver template prior to the replacement reaction.

A sampling of partially reacted structures with various crystallographic orientations and faceting reveals that the channel formation shown in Fig. 5 is not unique to the [211]-oriented structure shown, but is instead characteristic of substrate-based galvanic replacement processes on Au-coated silver templates. Figure 6 shows TEM images and SAED patterns for four sets of structures corresponding to the [211]-, [100]-, [111]-, and [110]-orientations. The images and SAED patterns for all similarly oriented structures have been rotated such that their crystallographic axes are aligned. Adjacent to the structures of each orientation is a stereographic projection (i.e., a Wulff net) showing the crystallographic directions for all low index planes. In this depiction the Miller index at the center corresponds to the crystallographic direction normal to the substrate while those at the outer extent correspond to in-plane directions. Intermediate values represent possibilities between these two extremes. An examination of the structures reveals that the channel consistently lies along one of the <110>-directions regardless of the faceting or structure orientation. Nanocage structures with the characteristic <111>-oriented pattern of openings were observed for the [100]- and [111]-orientations (denoted by white arrows in Figs. 6(h) and 6(l)).

Further insights regarding the galvanic replacement process are garnered from an examination of the underlying crystallography of the structures shown in Fig. 6. If the channels, as the data indicates, form preferentially along the in-plane <110>-directions then [211]-oriented templates present only one possible channel direction, i.e., along the in-plane [0$\bar{1}$1]-direction (Fig. 6(q)). This, however, is not the case for the [100]-oriented structures as two mutually perpendicular in-plane channel directions are possible (Fig. 6(r)). Noteworthy is the fact that the channel forms only along one of the two possible directions. Because these two channel directions are equivalent from a crystallographic standpoint, it follows that the choice between the two depends on factors other than the underlying crystallography of the template. The fact that a channel is also observed in a single direction for a [111]-oriented template (Fig. 6(i)) underscores this point as three different in-plane channel directions are possible for this orientation (Fig. 6(s)). Channels in [111]-oriented structures are, however, less well-defined and tend to hollow out one side of the structure before the other. Also noteworthy is the fact that partial channels are not typically observed for any orientation, a fact which suggests that Ag consumption is quite rapid once the channel begins to form. The [110]-oriented structures are unique in that they show channels in a variety of <110>-directions including the in-plane [$\bar{1}$10]-direction (Fig. 6(m)), at an angle of 60° relative to the substrate in the [01$\bar{1}$]-direction (Figs. 6(n) and 6(o)) and normal to the substrate in the [110]-direction (Fig. 6(p)). For this case, template faceting could play a decisive role in determining the channel direction. Another feature likely associated with faceting is the formation of much smaller channels (denoted by white arrows in Figs. 6(a) and 6(i)) in crystallographic directions consistent with <111>-oriented entry points. Such channels often appear in an in-plane direction normal to the main channel.

The planar defects observed for nanoshells derived from Au-coated silver templates formed on sapphire substrates (Fig. 1(d)) are also observed for nanoshells formed on the Si_3N_4 TEM grids. Figure 7 shows TEM images and the corresponding electron diffraction patterns for a silver template (Fig. 7(a)) and for nanoshells of various orientations (Figs. 4(b)–4(e)) which prominently exhibit this feature. For all cases the orientational relationship between the imaged structure and the diffraction pattern is consistent with the existence of stacking faults along a <111>-direction. The diffraction patterns also show the characteristic streaking expected along the stacking fault direction [31]. Both Ag and Au have low stacking fault energies [32, 33] and examples of the occurrence of this defect for nanoscale materials are frequent [34–36]. The origins of the stacking faults in the Ag template are likely

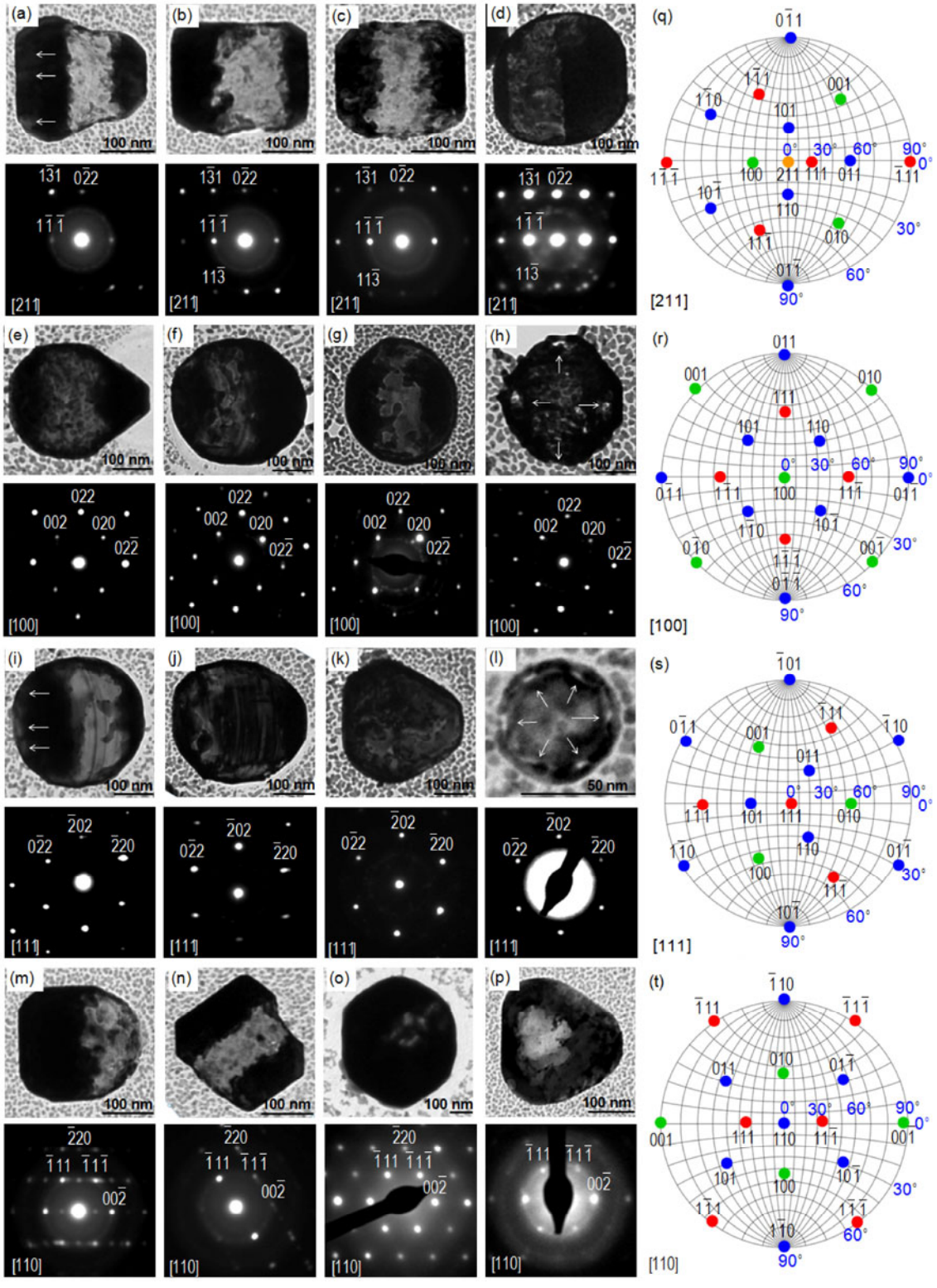

Figure 6 TEM images and the corresponding SAED patterns for structures derived from Au-coated silver templates with the (a)–(d) [211]-, (e)–(h) [100]-, (i)–(l) [111]-, and (m)–(p) [110]-orientation normal to the Si_3N_4 surface. To the right of each set of similarly oriented structures is (q)–(t) a stereographic projection showing the crystallographic directions for all the low index planes. It is noted that many of the imaged structures lie on top of the remnants of the thin discontinuous Au film because they have moved on the TEM grid during the drying process which occurs after the galvanic replacement reaction has been terminated.

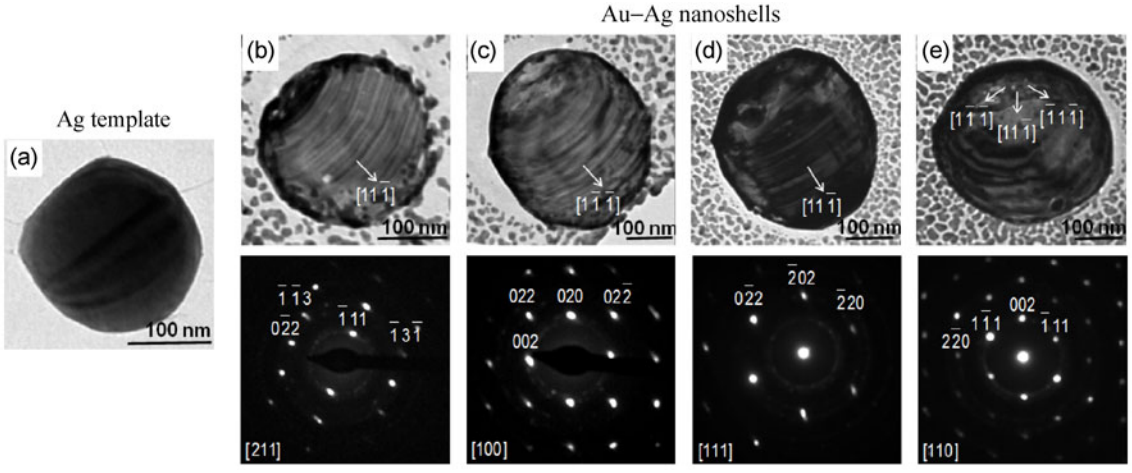

Figure 7 TEM images and the corresponding diffraction pattern for (a) a Ag template and for (b) [211]-, (c) [100]-, (d) [111]-, (e) [110]- oriented nanoshells showing prominent stacking faults along a <111>-direction.

associated with the relaxation of strains formed at the template–substrate interface [37, 38]. The result also suggests that the galvanic replacement process is amenable to defect transfer between the template and nanoshell. It is noted that the transfer of stacking faults from a Ag seed to a Ge nanowire has recently been demonstrated for a vapor-solid-solid growth mode [36]. Also noteworthy is that nanoscale fcc metals with stacking faults show enhanced mechanical properties due to the inhibition of dislocation motion [34, 39].

3 Discussion

3.1 Mechanisms guiding the hollowing process

The most notable result of the current investigation is that the hollow metal nanoshells derived from substrate-based galvanic replacement reactions can appear smooth or rough depending on whether or not the silver template is coated with a 3 nm thick layer of Au prior to its insertion into the reaction vessel. In order to rationalize this difference, it should first be noted that uncoated silver templates derived from colloidal processes often yield smooth nanoshells. This difference originates from the distinct nature of the substrate-based templates: They are larger and have properties which originate from the interfacial interactions which occur as the template assembles on the substrate at high temperatures. Such interactions: (i) Establish the crystallographic orientation, (ii) dictate the template shape through the establishment of contact angles which minimize the overall surface energy of the substrate–template combination and (iii) induce defect structures which minimize elastic strains originating from lattice mismatch. These influences lead to highly defected crystalline templates which, despite some faceting, appear quite rounded especially where facets intersect. Crystalline materials with rounded features show a step-terrace surface morphology on atomic length-scales [40]. Atoms at these step-edges are particularly reactive because of their lower coordination [41]. With step-edges, defects and certain facets all presenting highly reactive sites on rather large templates, the early stages of the galvanic replacement reaction are likely to be far more disorganized when compared to reactions carried out on templates with a highly faceted geometry (e.g., nanocubes). The surfaces of substrate-based templates could also be rendered more reactive than their colloidal counterparts due to the fact that they are free of surfactants. Such surface agents can alter both the rate and facet dependent nature of the replacement process [1, 42].

3.2 The uncoated silver template

The onset of the galvanic replacement reaction for the uncoated silver template will see the rapid oxidation of Ag as Au deposits on its surface. The fact that Au preferentially deposits on the high curvature surfaces where facets intersect is accounted for by the highly reactive nature of the step-edges [41] associated with such surfaces. This preferential deposition leads to

the formation of a nanoshell framework comprised of lobes which are disconnected and/or poorly connected at numerous locations. Lobe formation can be attributed, not only to preferential deposition, but also to the fact that this thin Au framework is intrinsically unstable to Rayleigh-like instabilities arising from thermal diffusion processes [43]. With a slower rate of Au deposition onto the {100} and {111} facets, there also exists favorable kinetics for the interdiffusion of subsurface Ag into the thin Au layer [2]. The galvanic replacement reaction will continue to hollow out the structure until the supply of pure Ag is exhausted. This reaction proceeds through the deposition of Au onto the outer shell cathode and the dissolution of Ag from the inner core anode. The deposition, however, is onto a surface that has been fundamentally transformed by early stage processes which result in: (i) A surface topography that is far from that of the pre-reacted template and (ii) local variations in the degree of Au–Ag alloying over the surface of the nanoshell. Both of these factors act as destabilizing influences in the later stages of the reaction which lead to the observed lobes and nanoshell porosity. Deviations in nanoscale curvature are well known to result in curvature-driven diffusion processes which act to lower the overall surface energy of the structure [44]. It should be noted that the nanoshell geometry is highly amenable to such surface diffusion processes as it allows for them to occur over both the inner and outer surfaces of the nanoshell. The resulting deterioration in nanoshell topography is further exacerbated by the dealloying of Ag-rich facets which leads to the injection of vacancies which, upon coalescence, rupture the surface of the nanoshell. It should be noted that important parallels can be drawn between these substrate-based galvanic replacement reactions on uncoated silver templates and the observed corrosion of Au–Ag alloys when exposed to electrolytic solutions which dissolve the Ag component [45–47]. Simulations by McCue et al. [41] are particularly relevant as they demonstrate that the step-edge topography exhibited by Au–Ag nanospheres gives rise to nanoscale porosity.

3.3 The Au-coated silver template

The evolution of the Au-coated silver template is different in that the galvanic replacement reaction begins at a point where the reactivity of the template surface has already been lowered by a 3 nm Au coating. The coating is particularly effective at lowering the reactivity of the step-edges as is evident from the nanoshells shown in Figs. 3(a), 3(c), 3(e), and 3(g), which clearly show that the deposition rate onto the {100} facets is nearly identical to that observed for the high curvature surfaces where facets intersect. The {111} facets, however, have a slower rate of reaction due to their low surface energy. Nevertheless, the overall topography of the structure is much smoother at every stage of the reaction due to the initial passivation of the template by the deposited Au. The fact that the surface is passivated prior to reaction is also expected to slow the initial stage of the reaction. In contrast to the case of the uncoated template, which presents a highly reactive surface, the passivated surface is one which must first be breached in order to expose a silver template anode from which the structure is efficiently hollowed.

The initial pitting of the Au-coated silver template is through a single opening (Fig. 2(e)), as is often observed in galvanic replacement reactions [14]. With few exceptions, the opening is near or at the base of the structure. Possible explanations for this location include: (i) A Au passivating layer that is thinner at the base due to the shadowing of the Au flux by the rounded template during the sputter deposition process or (ii) a higher number of defects near the template-substrate interface due to misfit dislocations. The choice of entry point along the circumference of the base is strongly influenced by the crystal structure of the template. It consistently results in the formation of a channel into the structure along a single <110>-direction regardless of the crystallographic orientation of the template relative to the underlying substrate. While it is not yet possible to detail the exact mechanisms guiding channel formation and evolution, several points of relevance can be made. First, the straightness of the channel is consistent with a dissolution process that proceeds in a layer-by-layer manner [45]. Second, the dissolution of silver from the channel walls is expected to be strongly connected to its coordination. In the bulk, each silver atom has a coordination number of 12. In an idealized

scenario, where surface reconstructions are ignored, the coordination numbers for atoms in {110}, {100}, and {111} surfaces are reduced to 7, 8, and 9, respectively. The lower coordination of atoms in {110} surfaces makes the addition of Au highly favorable because of the availability of unsatisfied bonds, a tendency that has been well-documented [1–4]. At the same time, Ag atoms that are a part of {110} surfaces are more prone to dissolution because they have the least number of nearest neighbor bonds. With {110} surfaces being an obvious choice for both deposition and dissolution, there exist two competing tendencies. In a scenario where a {110} surface of a silver template is exposed to the $HAuCl_4$ solution, Au will preferentially deposit on it. If, however, the replacement reaction proceeds by having electrons flowing between an anode on the inside of the structure to a cathode on the outside then the Au deposition is onto the outer shell and Ag^+ dissolution is from the inside surface of the template. In this scenario, Au^{3+} is not readily available for deposition on the inner surface. In this Au^{3+}-poor inner-shell environment a {110} surface, therefore, becomes the most favorable surface from which Ag^+ can dissolve. The mechanism by which a channel forms in a single <110>-direction when numerous equivalent channel directions are available remains ill-defined, but is likely related to the evolving charge distributions within the structure as it undergoes the reaction. Such effects are pronounced for galvanic replacement reactions carried out on Pd nanowires where electrons generated during Pd oxidation are forced to the ends of the nanowire where they reduce Au^{3+} to eventually form tadpole-like structures instead of the expected nanotube [22]. Such influences are also likely to play a role in the anisotropic hollowing observed in Ag–Au–Ag nanorod structures [48].

Once the supply of pure silver is exhausted, the nanoshells undergo a morphological reconstruction. The reconstruction is driven by the dealloying of the Ag in the Au–Ag nanoshell which results in the injection of vacancies into the nanoshell that leads to a gradual thinning and the subsequent rupture of the nanoshell walls. The observed nanocage openings in the <111>-directions during the dealloying process is common to galvanic replacement reactions [14]. The {111} facets are particularly amenable to such reconstructions, not only because they are thin, but because they are also likely to have a Ag content that is higher than the rest of the nanoshell since the early stage alloying process is expedited by the small amount of material being alloyed. The trend towards the formation of hexagonal openings reflects the six-fold symmetry of the {111}-planes. While hexagonal openings have not been previously observed in nanoshells derived from galvanic replacement reactions, it is noted that such features emerge in kinetic Monte Carlo simulations of the dealloying of bulk Au–Ag alloys [47].

3 Conclusion

We have demonstrated that the early stages of substrate-based galvanic replacement reactions lead to late stage instabilities which give rise to a morphological deconstruction of the nanoshells produced. By merely coating the outer surface of the sacrificial template with a thin layer of Au prior to reaction we inhibit these instabilities, fundamentally altering the product of the reaction. In contrast to the porous, rough nanoshells derived from the uncoated template, the Au layer leads to the formation of hollow Au–Ag nanoshells which are smooth, robust and crystalline and which exhibit a well-defined pattern of geometric openings. We attribute these differences to the passivation of the highly reactive surface of the silver template by the Au layer. In the absence of this passivating layer, the surface topography of the emerging nanoshell is dramatically altered by the highly reactive nature of curved surfaces of the sacrificial template. This gives rise to a nanoshell with a weak structural framework that is unable to withstand the destabilizing influences of dealloying and thermal diffusion processes. Surface passivation, however, prevents these destabilizing influences, allowing for the orderly dissolution of the template from a single pit at its base. Unique to these studies is the observation that the hollowing initiates in a <110>-direction and proceeds first through the rapid dissolution of a single channel across the entire extent of the template followed by the removal of the remaining Ag. This observation is attributed to the combined influences of atoms in {110}-surfaces having

low coordination, the Au^{3+}-poor environment within the interior of the hollowing shell and a reaction that proceeds through the transfer of electrons from an inner shell anode to an outer shell cathode. The final stages of the reaction lead to the formation of openings in the <111>-directions where each template orientation relative to the underlying substrate yields a unique nanocage geometry. Collectively, these synthetic and mechanistic findings demonstrate the critical importance of template engineering in substrate-based galvanic replacement reactions.

4 Methods

4.1 Nanoshell/nanocage array fabrication

Periodic arrays of sacrificial Ag templates were fabricated on 10 mm × 8 mm × 0.5 mm (0001)-oriented sapphire substrates (MTI Corp.) using a lithography-free route described elsewhere [25]. Briefly, a shadow mask with a periodic array of 900 nm diameter openings and a pitch of 1.6 μm was used to define 75 nm high antimony pedestals topped with a 45 nm thick layer of Ag. Heating the structures to 750 ˚C in 13 min resulted in pedestal annihilation through evaporation/sublimation that led to a forced agglomeration of Ag atoms at the center of each pedestal. Continued heating to 850 ˚C in 4 min, where it held for 10 min, caused the templates to become more faceted, but where 70% of the Ag was lost in the process through sublimation. Galvanic replacement reactions were then carried out on these Ag templates as well as on identical templates which were first sputter coated (Model 681 Gatan High Resolution Ion Beam Coater) with 3 nm of Au prior to reaction. A typical reaction proceeded by placing the substrate into a 20 μM $HAuCl_4$ (Alfa Aesar) solution heated to 100 ˚C for 10 min, after which it was slowly pulled out of the solution and dried.

4.2 TEM sample preparation

Two procedures were devised in order to simplify TEM sample preparation: (i) The transfer of the nanoshells from the substrate surface to TEM grids was carried out by first dipping the sapphire substrate into acetone and then, upon removal, placing a holey carbon TEM grid (Quantifoil) facedown over the nanoshells. As the acetone dries, capillary forces pull the grid towards the structures, ultimately forming bonds between the two surfaces. As the grid is removed from the substrate many of the nanoshells are peeled off the sapphire surface leaving them inverted in a nanobowl configuration. The number of nanoshells sticking to the grid can be significantly increased by limiting the exposure of the nanoshell to air and through the sputter deposition of a few nanometers of Au onto the grid immediately prior to use. Both of these procedures likely increase the number of bonds shared between the TEM grid and the nanoshell. (ii) Randomly positioned silver templates were assembled directly on Si_3N_4 TEM grids (Ted Pella, Inc.). The processing route used to form the silver templates is described in detail elsewhere [49]. Briefly, continuous thin films of Sb (12 nm) and Ag (18 nm) were sputter deposited over the surface of the TEM grid. The grid was then exposed to a heating regimen which caused the Ag atoms to agglomerate into islands, but where the concurrent sublimation of antimony greatly enhances the agglomeration process. The grid with templates was then exposed to the galvanic replacement reaction.

4.3 Instrumentation

SEM images were obtained in secondary electron mode using either an FEI Quanta 400 or a 600 FEG ESEM. The samples were coated with a gold–palladium film to improve imaging. TEM images were obtained using an FEI Tecnai 12T Transmission Electron Microscope.

Acknowledgements

This work is funded by the National Science Foundation (NSF) (No. DMR-1053416) The Faculty Early Career Development (CAREER) Award to SN. The authors also acknowledge the expertise of Dr. F. Monson (Technical Director, Center for Microanalysis, Imaging, Research and Training, West Chester University). The work has benefited from the facilities available through Temple University's Material Research

Facility (MRF) and the Penn Regional Nanotechnology Facility. K.D.G. acknowledges support received through a Temple University Graduate Student Fellowship.

Electronic Supplementary Material: Supplementary material (additional characterization which shows: (i) The homogeneity of Au passivation layers, (ii) that slower reaction rates on uncoated templates yield rough structures, and (iii) the alignment of channels in adjacent structures) is available in the online version of this article at http://dx.doi.org/10.1007/s12274-013-0402-y

References

[1] Xia, X. H.; Wang, Y.; Ruditskiy, A.; Xia, Y. N. Galvanic replacement: A simple and versatile route to hollow nanostructures with tunable and well-controlled properties. *Adv. Mater.* **2013**, *25*, 6313–6333.

[2] Cobley, C. M.; Xia, Y. N. Engineering the properties of metal nanostructures via galvanic replacement reactions. *Mater. Sci. Eng. R* **2010**, *70*, 44–62.

[3] Yin, Y. D.; Erdonmez, C.; Aloni, S.; Alivisatos, A. P. Faceting of nanocrystals during chemical transformation: From solid silver spheres to hollow gold octahedra. *J. Am. Chem. Soc*. **2006**, *128*, 12671–12673.

[4] Zhang, Q. B.; Xie, J. P.; Lee, J. Y.; Zhang, J. X.; Boothroyd, C. Synthesis of Ag@AgAu metal core/alloy shell bimetallic nanoparticles with tunable shell compositions by a galvanic replacement reaction. *Small* **2008**, *4*, 1067–1071.

[5] Yu, Y.; Zhang, Q. B.; Xie, J. P.; Lee, J. Y. Engineering the architectural diversity of heterogeneous metallic nanocrystals. *Nat. Commun.* **2013**, *4*, 1454.

[6] Skrabalak, S. E.; Au, L.; Li, X. D.; Xia, Y. N. Facile synthesis of Ag nanocubes and Au nanocages. *Nat. Protoc.* **2007**, *2*, 2182–2190.

[7] Chen, J. Y.; Yang, M. X.; Zhang, Q.; Cho, E. C.; Cobley, C. M.; Kim, C.; Glaus, C.; Wang, L. H. V.; Welch, M. J.; Xia, Y. N. Gold nanocages: A novel class of multifunctional nanomaterials for theranostic applications. *Adv. Funct. Mater* **2010**, *20*, 3684–3694.

[8] Xia, Y. N.; Halas, N. J. Shape-controlled synthesis and surface plasmonic properties of metallic nanostructures. *MRS Bull.* **2005**, *30*, 338–348.

[9] Sun, Y. G.; Xia, Y. N. Increased sensitivity of surface plasmon resonance of gold nanoshells compared to that of gold solid colloids in response to environmental changes. *Anal. Chem*. **2002**, *74*, 5297–5305.

[10] Sun, Y. G.; Mayers, B.; Xia, Y. N. Metal nanostructures with hollow interiors. *Adv. Mater.* **2003**, *15*, 641–646.

[11] Fu, E.; Ramsey, S. A.; Chen, J. Y.; Chinowsky, T. M.; Wiley, B.; Xia, Y. N.; Yager, P. Resonance wavelength-dependent signal of absorptive particles in surface plasmon resonance-based detection. *Sens. Actuators* **2007**, *123*, 606–613.

[12] Kim, S. W.; Kim, M.; Lee, W. Y.; Hyeon, T. Fabrication of hollow palladium spheres and their successful application to the recyclable heterogeneous catalyst for Suzuki coupling reactions. *J. Am. Chem. Soc*. **2002**, *124*, 7642–7643.

[13] Yu, X. F.; Wang, D. S.; Peng, Q.; Li, Y. D. High performance electrocatalyst: Pt–Cu hollow nanocrystals. *Chem. Commun.* **2011**, *47*, 8094–8096.

[14] Sun, Y. G.; Xia, Y. N. Mechanistic study on the replacement reaction between silver nanostructures and chloroauric acid in aqueous medium. *J. Am. Chem. Soc*. **2004**, *126*, 3892–3901.

[15] Lu, X. M.; Tuan, H. Y.; Chen, J. Y.; Li, Z. Y.; Korgel, B. A.; Xia, Y. Mechanistic studies on the galvanic replacement between multiply twinned particles of Ag and $HAuCl_4$ in an organic medium. *J. Am. Chem. Soc*. **2007**, *129*, 1733–1742.

[16] Sun, Y. G.; Wang, Y. X. Monitoring galvanic replacement reaction between silver nanowires and $HAuCl_4$ by *in situ* transmission X-ray microscopy. *Nano Lett.* **2011**, *11*, 4386–4392.

[17] Ott, A.; Bhargava, S. K.; O'Mullane, A. P. A study of the galvanic replacement reaction at surfaces and the role of lateral charge propagation. *Surf. Sci*. **2012**, *606*, L5–L9.

[18] Cobley, C. M.; Zhang, Q.; Song, W.; Xia, Y. N. The role of surface nonuniformity in controlling the initiation of a galvanic replacement reaction. *Chem. Asian J.* **2011**, *6*, 1479–1484.

[19] Sun, Y. G.; Mayers, B. T.; Xia, Y. N. Template-engaged replacement reaction: A one-step approach to the large-scale synthesis of metal nanostructures with hollow interiors. *Nano Lett.* **2002**, *2*, 481–485.

[20] Skrabalak, S. E.; Chen, J. Y.; Sun, Y. G.; Lu, X. M.; Au, L.; Cobley, C. M.; Xia, Y. N. Gold nanocages: Synthesis, properties, and applications, *Acc. Chem. Res.* **2008**, *41*, 1587–1595.

[21] Kim, M. H.; Lu, X. M.; Wiley, B.; Lee, E. P.; Xia, Y. N. Morphological evolution of single-crystal Ag nanospheres during the galvanic replacement reaction with $HAuCl_4$. *J. Phys. Chem. C* **2008**, *112*, 7872–7876.

[22] Camargo, P. H. C.; Xiong, Y. J.; Ji, L.; Zuo, J. M.; Xia, Y. N. Facile synthesis of tadpole-like nanostructures consisting of Au heads and Pd tails. *J. Am. Chem. Soc.* **2007**, *129*, 15452–15453.

[23] Henry, C. R. Morphology of supported nanoparticles. *Prog. Surf. Sci.* **2005**, *80,* 92–116.

[24] Gilroy, K. D.; Farzinpour, P.; Sundar, A.; Tan, T.; Hughes, R. A.; Neretina, S. Substrate-based galvanic replacement reactions carried out on heteroepitaxially formed silver templates. *Nano Res.* **2013**, *6*, 418–428.

[25] Farzinpour, P.; Sundar, A.; Gilroy, K. D.; Eskin, Z. E.; Hughes, R. A.; Neretina, S. Dynamic templating: A large area processing route for the assembly of periodic arrays of sub-micrometer and nanoscale structures. *Nanoscale* **2013**, *5*, 1929–1938.

[26] Ridelman, Y.; Singh, G.; Popovitz-Biro, R.; Wolf, S. G.; Das, S.; Klajn, R. Metallic nanobowls by galvanic replacement reaction on heterodimeric nanoparticles. *Small* **2012**, *8*, 654–660.

[27] Rao, Y. Y.; Tao, Q.; An, M.; Rong, C. H.; Dong, J.; Dai, Y. R.; Qian, W. P. Novel and simple route to fabricate 2D ordered gold nanobowl arrays based on 3D colloidal crystals. *Langmuir* **2011**, *27*, 13308–13313.

[28] Li, X. L.; Zhang, Y. Z.; Shen, Z. X.; Fan, H. J. Highly ordered arrays of particle-in-bowl plasmonic nanostructures for surface enhanced Raman scattering. *Small* **2012**, *8,* 2548–2554.

[29] Ye, J.; Van Dorpe, P.; Van Roy, W.; Borghs, G.; Maes, G. Fabrication, characterization, and optical properties of gold nanobowl submonolayer structures. *Langmuir* **2009**, *25,* 1822–1827.

[30] Vitos, L.; Ruban, A. V.; Skriver, H. L.; Kollár, J. The surface energy of metals. *Surf. Sci.* **1998**, *411*, 186–202.

[31] Li, B.; Yan, P. F.; Sui, M. L.; Ma, E. Transmission electron microscopy study of stacking faults and their interaction with pyramidal dislocations in deformed Mg. *Acta Mater.* **2010**, *58*, 173–179.

[32] Mehl, M. J.; Papaconstantopoulos, D. A.; Kioussis, N.; Herbranson, M. Tight-binding study of stacking fault energies and the Rice criterion of ductility in the fcc metals. *Phys. Rev. B* **2000**, *61*, 4894–4897.

[33] Lee, B. J.; Shim, J. H.; Baskes, M. I. Semiempirical atomic potentials for the fcc metals Cu, Ag, Au, Ni, Pd, Pt, Al, and Pb based on first and second nearest-neighbor modified embedded atom method. *Phys. Rev. B* **2003**, *68*, 144112.

[34] Wang, J. G.; Tian, M. L.; Mallouk, T. E.; Chan, M. H. W. Microtwinning in template-synthesized single-crystal metal nanowires. *J. Phys. Chem. B* **2004**, *108*, 841–845.

[35] Lofton, C.; Sigmund, W. Mechanisms controlling crystal habits of gold and silver colloids. *Adv. Funct. Mater.* **2005**, *15*, 1197–1208.

[36] Barth, S.; Boland, J. J.; Holmes, J. D. Defect transfer from nanoparticles to nanowires. *Nano Lett.* **2011**, *11*, 1550–1555.

[37] Moewe, M.; Chuang, L. C.; Dubrovskii, V. G.; Chang-Hasnain, C. Growth mechanisms and crystallographic structure of InP nanowires on lattice-mismatched substrates. *J. Appl. Phys.* **2008**, *104*, 044313.

[38] Wang, Y.; Liao, Z.; Xu, H. Y.; Xiu, F. X.; Kou, X. F.; Wang, Y.; Wang, K. L.; Drennan, J.; Zou, J. Structural evolution of GeMn/Ge superlattices grown by molecular epitaxy under different growth conditions. *Nanoscale Res. Lett.* **2011**, *6*, 624.

[39] Merz, M. D.; Dahlgren, S. D. Tensile strength and work hardening of ultrafine-grained high-purity copper. *J. Appl. Phys.* **1975**, *46*, 3235–3237.

[40] Ohnishi, H.; Kondo, Y.; Takayanagi, K. UHV electron microscope and simultaneous STM observation of gold stepped surfaces. *Surf. Sci.* **1998**, *415*, L1061–L1064.

[41] McCue, I.; Snyder, J.; Li, X.; Chen, Q.; Sieradzki, K.; Erlebacher, J. Apparent inverse Gibbs–Thomson effect in dealloyed nanoporous nanoparticles. *Phys. Rev. Lett.* **2012**, *108*, 225503.

[42] Sau, T. K.; Rogach, A. L. Nonspherical noble metal nanoparticles: Colloid-chemical synthesis and morphology control. *Adv. Mater.* **2010**, *22*, 1781–1804.

[43] Kim, D.; Giermann, A. L.; Thompson, C. V. Solid-state dewetting of patterned thin films. *Appl. Phys. Lett.* **2009**, *95*, 251903.

[44] Thompson, C. V. Solid-state dewetting of thin films. *Ann. Rev. Mater. Res.* **2012**, *42*, 399–434.

[45] Erlebacher, J.; Aziz, M. J.; Karma, A.; Dimitrov, N.; Sieradzki, K. Evolution of nanoporosity in dealloying. *Nature* **2001**, *410*, 450–453.

[46] Erlebacher, J.; Seshadri, R. Hard materials with tunable porosity. *MRS Bull.* **2009**, *34*, 561–568.

[47] Erlebacher, J. An atomistic description of dealloying: Porosity evolution, the critical potential, and rate-limiting behavior. *J. Electrochem. Soc.* **2004**, *151*, C614–C626.

[48] Seo, D.; Song, H. Asymmetric hollow nanorod formation through a partial galvanic replacement reaction. *J. Am. Chem. Soc.* **2009**, *131*, 18210–18211.

[49] Farzinpour, P.; Sundar, A.; Gilroy, K. D.; Eskin, Z. E.; Hughes, R. A.; Neretina, S. Altering the dewetting characteristics of ultrathin gold and silver films using a sacrificial antimony layer. *Nanotechnology* **2012**, *23*, 495604.